

Bridging Cognitive Neuroscience and Graph Intelligence: Hippocampus-Inspired Multi-View Hypergraph Learning for Web Finance Fraud

Rongkun Cui
Tongji University
Shanghai, China
jokercui@tongji.edu.cn

Kun Zhu*
Tongji University
Shanghai, China
kzhu00@tongji.edu.cn

Nana Zhang
Donghua University
Shanghai, China
nnzhang@dhu.edu.cn

Qi Zhang
Tongji University
Shanghai, China
zhangqi_cs@tongji.edu.cn

Abstract

Online financial services constitute an essential component of contemporary web ecosystems, yet their openness introduces substantial exposure to fraud that harms vulnerable users and weakens trust in digital finance. Such threats have become a significant web harm that erodes societal fairness and affects the well-being of online communities. However, existing detection methods based on graph neural networks (GNNs) struggle with two persistent challenges: (1) fraud camouflage, where malicious transactions mimic benign behaviors to evade detection, and (2) long-tailed data distributions, which obscure rare but critical fraudulent cases. To fill these gaps, we propose HIMVH, a Hippocampus-Inspired Multi-View Hypergraph learning model for web finance fraud detection. Specifically, drawing inspiration from the scene conflict monitoring role of the hippocampus, we design a cross-view inconsistency perception module that captures subtle discrepancies and behavioral heterogeneity across multiple transaction views. This module enables the model to identify subtle cross-view conflicts for detecting online camouflaged fraudulent behaviors. Furthermore, inspired by the match–mismatch novelty detection mechanism of the CA1 region, we introduce a novelty-aware hypergraph learning module that measures feature deviations from neighborhood expectations and adaptively reweights messages, thereby enhancing sensitivity to online rare fraud patterns in the long-tailed settings. Extensive experiments on six web-based financial fraud datasets demonstrate that HIMVH achieves 6.42% improvement in AUC, 9.74% in F1 and 39.14% in AP on average over 15 SOTA models.

*Corresponding author.

Permission to make digital or hard copies of all or part of this work for personal or classroom use is granted without fee provided that copies are not made or distributed for profit or commercial advantage and that copies bear this notice and the full citation on the first page. Copyrights for components of this work owned by others than the author(s) must be honored. Abstracting with credit is permitted. To copy otherwise, or republish, to post on servers or to redistribute to lists, requires prior specific permission and/or a fee. Request permissions from permissions@acm.org.

WWW'26, Dubai, United Arab Emirates

© 2026 Copyright held by the owner/author(s). Publication rights licensed to ACM. ACM ISBN 978-x-xxxx-xxxx-x/YYY/MM
https://doi.org/XXXXXXX.XXXXXXX

CCS Concepts

- Information systems → Data mining; • Social and professional topics → Economic impact.

ACM Reference Format:

Rongkun Cui, Nana Zhang, Kun Zhu, and Qi Zhang. 2026. Bridging Cognitive Neuroscience and Graph Intelligence: Hippocampus-Inspired Multi-View Hypergraph Learning for Web Finance Fraud. In *Proceedings of The Web Conference 2026 (WWW'26)*. ACM, New York, NY, USA, 11 pages. <https://doi.org/XXXXXXX.XXXXXXX>

1 Introduction

Web finance has become a critical part of digital life and provides essential channels for credit access and fund movement across web communities. This shift creates new forms of exposure to financial harm, as web transaction networks allow fraudulent behavior to propagate across services and reach large populations. This problem now stands as a major web harm with real societal consequences, since web finance fraud reduces trust in digital public infrastructure, erodes societal fairness by intensifying the disadvantages faced by groups with restricted financial capacity, and intensifies existing economic vulnerability [1, 16, 30, 51]. As financial interactions across the web grow more complex and interlinked, the need for reliable intelligence systems that counter online fraud becomes a central requirement for a safe and fair society.

In response to the substantial societal impact of web finance fraud, extensive research [6, 17, 34] has been conducted to develop models capable of accurately identifying online fraudulent transactions. Initial methods used rule-based heuristics but were gradually replaced by traditional machine learning (e.g., decision trees) [25, 53]. As large-scale online transactions grow, deep learning techniques gain more popularity due to their capability to capture complex patterns [38]. With the growing sophistication of online fraudulent behaviors [28], graph neural networks (GNNs) have become a mainstream paradigm in web finance fraud detection due to their capability to capture and learn from the intricate relational structures embedded within web-based financial systems [13, 15].

Nevertheless, these web finance fraud detection methods based on GNNs still suffer from two significant limitations: (1) **Imitation-based camouflaged fraud**. These fraudulent transactions deliberately imitate legitimate behaviors and thus become difficult to

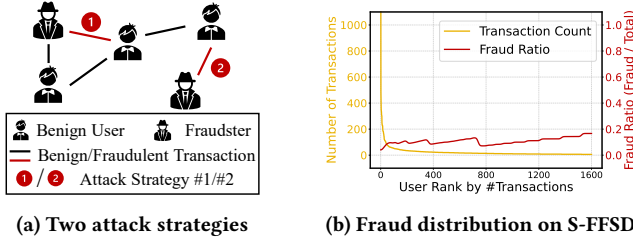


Figure 1: (a) Two attack strategies targeting the head and tail of the distribution. (b) Fraud distribution on the S-FFSD dataset.

distinguish with conventional graph patterns [11, 46]. (2) **Reduced detectability of fraudulent instances in the distribution tail.** Fraud in the tail of the distribution is rare and atypical, with limited representative samples. This scarcity hinders effective learning and causes models to overlook subtle yet critical fraud [12]. As illustrated in Figure 1 (a), attack strategy #2 targets sparse regions of the transaction graph, which correspond to the tail of data distribution. With limited structural context, these regions are more vulnerable to undetected attacks [23]. As shown in Figure 1 (b), the distribution in the S-FFSD dataset reveals a higher fraud ratio in tail regions, and highlights the greater risk in low-density areas. The aforementioned challenges remain inadequately addressed. In this context, brain-inspired intelligence emerges as a compelling alternative, offering a biologically grounded foundation for contextual understanding, adaptive learning, and resilience against uncertainty. These capabilities are crucial for detecting sophisticated fraudulent behaviors in web-based financial systems.

Motivated by the aforementioned brain-inspired intelligence, we propose HIMVH, a Hippocampus-Inspired Multi-View Hypergraph learning model to detect web finance fraud. Figure 2 presents the two hippocampal mechanisms that serve as the foundation of our model, which will be elaborated in detail in the Preliminaries section. To capture high-order interactions in complex online transactions, we build a multi-view hypergraph where each hyperedge encodes context-aware group relations across views. Based on this, a hippocampal discrepancy perception mechanism is designed to identify latent cross-view inconsistencies in camouflaged fraud. Furthermore, a novelty-aware hypergraph neural network, inspired by the match–mismatch novelty detection in CA1 region, estimates prediction deviations within local neighborhoods and amplifies fraud responses to detect rare fraud patterns in long-tailed distributions. The main contributions can be summarized as follows:

- We propose HIMVH, the first work to reformulate the message-passing mechanism in graph learning through a brain-inspired perspective. We develop a CA1-inspired novelty-aware hypergraph network that quantifies local feature deviations to adaptively reweight messages, and enhance the representation of sparse minority samples under long-tailed distributions.
- We design a hippocampal cross-view discrepancy perception module that systematically captures latent conflicts and heterogeneity of camouflaged online transactions across multiple views.

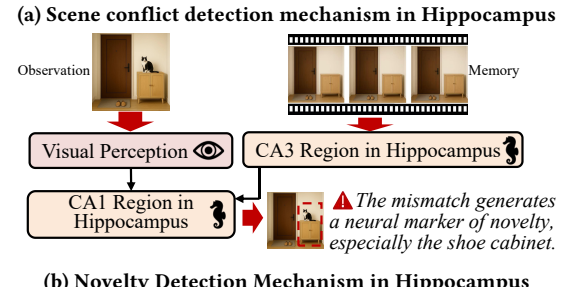
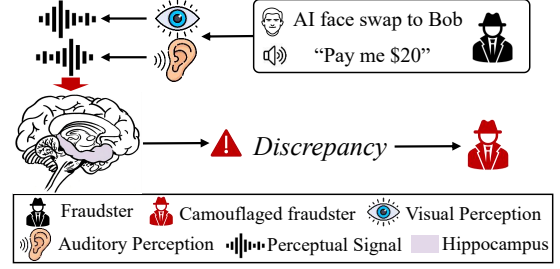


Figure 2: Two mechanisms in hippocampus.

- Experimental results on six web finance fraud datasets underscore the HIMVH's superiority, which achieves an average improvement of 6.42% in AUC, 9.74% in F1 score, and 39.14% in AP compared to 15 SOTA models.

2 Related Work

2.1 Web Finance Fraud Detection

During the initial stages of web finance fraud detection, traditional machine learning techniques were predominantly employed [27, 29]. Ensemble methods such as GBT [31, 43, 52] provide competitive accuracy by aggregating weak learners, and allow them to handle large-scale, highly imbalanced datasets while maintaining robustness to noisy transactional patterns.

The emergence of deep learning has led to a paradigm shift in web finance fraud detection. Conventional machine learning techniques were replaced by advanced architectures such as LSTM, RNN, and CNN, which demonstrate stronger representational capacity for complex financial signals. These models [38, 42, 47] deliver performance by accurately modeling temporal dependencies, sequential dynamics, and localized features within online transactional data. They also reveal subtle and irregular behavioral patterns that remain obscure to traditional approaches, which allows a more accurate assessment of hidden and evolving fraud risks.

However, traditional deep learning models still treat online transactions as independent samples and overlook cross-entity relationships. This limitation reduces their capability to capture coordinated or camouflaged fraud. As a result, researchers increasingly adopt GNNs, which model structural dependencies and multi-hop interaction patterns to reveal sophisticated web-based fraudulent behaviors more effectively.

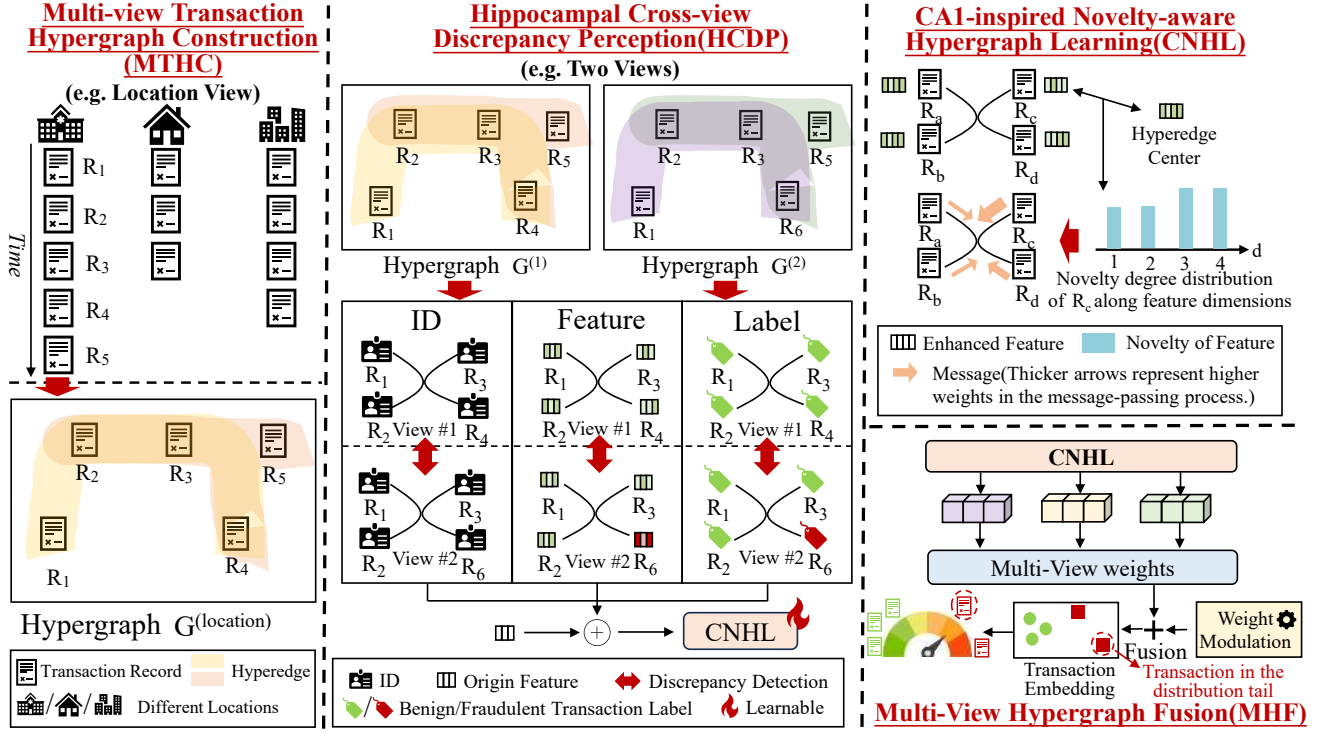


Figure 3: Overview of the proposed HIMVH model.

2.2 Graph-based Financial Risk Control

Graph learning has proven highly effective [26, 41] in detecting web finance fraud by modeling the structural dependencies between entities [24]. SA-GNN [20] builds graphs via selective representation and dual similarity constraints based on features and labels. Semi-GNN [37] employs a hierarchical attention mechanism to model diverse transaction behaviors. SplitGNN [40] partitions the graph through edge classification and introduces adaptive filters to enhance representation for fraud-related anomalies. ASA-GNN [33] learns discriminative embeddings and samples informative neighbors to suppress noise. HHSgt [39] employs a relation-aware sparse graph transformer and addresses the structural heterogeneity observed in financial fraud graphs. MTPNet [10] builds transaction graphs at multiple temporal scales and applies adaptive neighborhood aggregation to highlight the most relevant behavioral cues, which ultimately leads to more accurate detection of fraudulent activities. FraudGCN [36] constructs a heterogeneous corporate network to integrate industrial, supply chain, and audit-sharing relationships. Moreover, it employs a graph encoder with relation-wise aggregation and attention fusion, supplemented by a diffusion-based sampling strategy and focal loss to handle class imbalance.

Nonetheless, these models provide limited support for uncovering imitation-based online fraudulent behaviors and lack dedicated mechanisms to effectively identify infrequent yet critical fraud instances in the tail of long-tailed distributions.

3 Preliminaries

3.1 Scene Conflict Detection Mechanism

Scene conflict detection in hippocampus involves identifying inconsistencies across sensory inputs originating from distinct modalities [14]. This enables hippocampus system to resolve spatial or contextual conflicts by integrating mismatched elements into a coherent scene representation.

For instance, when an individual hears a familiar voice but visually identifies an unfamiliar face, the conflict between auditory and visual modalities may trigger the hippocampal scene conflict detection. This process enables the brain to reconcile incongruent sensory inputs and identify potentially deceptive or incongruent environmental cues.

3.2 Match–Mismatch Novelty Detection Mechanism

In the hippocampal CA3 region, the brain forms predictions about sensory inputs based on memory representations. When actual inputs deviate from these predictions, CA1 region generates a mismatch response [2], which serves as a neural marker of novelty, highlighting rare and unexpected patterns in the environment.

For example, when going home each day, CA3 predicts the familiar scene at the apartment entrance. If the sensory input matches this expectation, CA1 remains relatively inactive. However, if a cat unexpectedly appears on the shoe cabinet, CA1 generates a strong mismatch response, signaling novelty. Following such an event, one may begin to wonder whether a cat will appear at the apartment

entrance each day and allocate heightened attention to a previously inconspicuous element, namely the shoe cabinet.

4 Methodology

In this section, we introduce the details of HIMVH. As shown in Figure 3, HIMVH consists of four modules: multi-view transaction hypergraph construction module, hippocampal cross-view discrepancy perception module, CA1-inspired novelty-aware hypergraph learning module, multi-view hypergraph fusion module.

4.1 Multi-view Transaction Hypergraph Construction

We first introduce the Multi-view Transaction Hypergraph Construction (MTHC) module. Specifically, we construct distinct views of the online transaction data based on different attribute columns such as sender ID, receiver ID, transaction location, and transaction type, each serving as a view-specific key. For each view, we build undirected hypergraphs by applying a temporal sliding window over chronologically ordered transactions.

For a given view-specific key key_a , we define the corresponding view a as an undirected hypergraph $\mathcal{G}^{(a)} = (\mathcal{V}^{(a)}, \mathcal{E}^{(a)})$, where $\mathcal{V}^{(a)}$ denotes the set of nodes, with each node representing an individual transaction. The set of hyperedges $\mathcal{E}^{(a)}$ is constructed such that transactions falling within the same temporal sliding window form a hyperedge. In the following, we provide a detailed description of the hyperedge construction process in view a .

$$\forall c \in C_a, \mathcal{V}_c^a = Sort_{time}(\{v_i \in \mathcal{V} | Cate^a(v_i) = c\}), \quad (1)$$

where \mathcal{A} denotes the set of all views, and for each view $a \in \mathcal{A}$, C_a represents the set of unique categories under view a (i.e., view-specific key key_a). \mathcal{V}_c^a denotes the set of transactions belonging to category c , sorted in ascending order by their transaction timestamps.

$$e_{c,j}^a = \{v_{c_j}, v_{c_{j+1}}, \dots, v_{c_{j+w-1}}\}, j = 1, 2, \dots, |\mathcal{V}_c^a| - w + 1, \quad (2)$$

where $e_{c,j}^a$ denotes the j -th hyperedge constructed under view a for category c , and w is a hyperparameter that defines the size of the temporal sliding window, corresponding to the number of nodes contained within each hyperedge.

Therefore, the hyperedge set under view a is defined as:

$$\mathcal{E}^{(a)} = \bigcup_{c \in C_a} \bigcup_j e_{c,j}^a. \quad (3)$$

4.2 Hippocampal Cross-view Discrepancy Perception

As introduced in the Preliminaries, the hippocampus integrates cues from different sources and detects inconsistencies to identify web finance fraud. Inspired by its scene conflict detection mechanism, we propose a Hippocampal Cross-view Discrepancy Perception (HCDP) module to detect camouflaged fraud. Although fraudsters may mimic normal transaction behavior, certain attributes such as transaction location or IP address are difficult to manipulate. This leads to inconsistencies across views, which the HCDP module captures to reveal subtle signs of deception.

We design multi-dimensional metrics to quantify the inconsistencies of the same transaction node across different views, including identity (ID_Diff), feature ($Feat_Diff$), and label discrepancy ($Label_Diff$).

$$ID_Diff_i^{(a_1, a_2)} = 1 - \frac{|\mathcal{N}_i^{a_1} \cap \mathcal{N}_i^{a_2}|}{|\mathcal{N}_i^{a_1} \cup \mathcal{N}_i^{a_2}|}, \quad (4)$$

where $\mathcal{N}_i^{a_1}$ and $\mathcal{N}_i^{a_2}$ denote the sets of neighboring nodes of node i in views a_1 and a_2 , respectively. The term $ID_Diff_i^{(a_1, a_2)}$ measures the structural discrepancy of node i across views a_1 and a_2 , and is computed as the Jaccard distance between its two neighbor sets.

$$p_i^a = \text{Softmax}(\text{Mean}(\{x_j | j \in \mathcal{N}_i^a\})), \quad (5)$$

$$Feat_Diff_i^{(a_1, a_2)} = \frac{1}{2} \cdot KL(M||p_i^{a_1}) + \frac{1}{2} \cdot KL(M||p_i^{a_2}), \quad (6)$$

where x_j is the feature of neighbor j under view a , and p_i^a represents the distribution of neighboring features. In Eq. (6), $Feat_Diff_i^{(a_1, a_2)}$ denotes the feature discrepancy between views a_1 and a_2 with Jensen–Shannon divergence, and M is the average of the two distributions $p_i^{a_1}$ and $p_i^{a_2}$.

$$\mathcal{H}_i^a = - \sum_{label \in \{0, 1\}} r_{i,label}^a \cdot \log(r_{i,label}^a + \epsilon), \quad (7)$$

$$Label_Diff_i^{(a_1, a_2)} = |\mathcal{H}_i^{a_1} - \mathcal{H}_i^{a_2}|, \quad (8)$$

where \mathcal{H}_i^a denotes the label entropy of node i under view a , and $r_{i,label}^a$ is the empirical probability of each label (0 for normal, 1 for fraudulent) among its neighbors. $Label_Diff_i^{(a_1, a_2)}$ reflects the inconsistency of local label distributions between views a_1 and a_2 .

$$h_i = \text{Concat}\left[x_i, \frac{1}{\binom{|\mathcal{A}|}{2}} \sum_{j < k} ID_Diff_i^{(a_j, a_k)}, \frac{1}{\binom{|\mathcal{A}|}{2}} \sum_{j < k} Feat_Diff_i^{(a_j, a_k)}, \frac{1}{\binom{|\mathcal{A}|}{2}} \sum_{j < k} Label_Diff_i^{(a_j, a_k)}\right], \quad (9)$$

where h_i denotes the enhanced representation of node i , formed by concatenating its original feature x_i with three types of cross-view discrepancy metrics: identity, feature, and label discrepancy. Each discrepancy term is computed by averaging over all $\binom{|\mathcal{A}|}{2}$ unordered pairs of views.

4.3 CA1-inspired Novelty-aware Hypergraph Learning

Inspired by the match–mismatch novelty detection in the Preliminaries, we propose the CA1-inspired Novelty-aware Hypergraph Learning (CNHL) module, a heterophily-sensitive graph learning paradigm. It adaptively reweights messages based on local deviation to enhance the representation of long-tailed samples. We illustrate it by detailing a single layer of CNHL.

$$\mu_e = \frac{1}{w} \sum_{i \in e} h_i, \quad (10)$$

where w denotes both the temporal window size and the number of nodes within hyperedge e , and μ_e represents the hyperedge center of all w nodes. The center serves as an analogy to the predictive pattern generated by CA3 region. It is noted that HIMVH incorporates

label propagation for semi-supervised scenarios, with label embeddings for labeled nodes and zero embeddings for unlabeled ones, with h_i formed by fusing original features and label embeddings.

$$Var_l = \frac{1}{k} \sum_{i \in e} (h_{i,l} - \mu_{e,l})^2, \quad (11)$$

$$g_l = \frac{\exp(\beta \cdot Var_l)}{\sum_{m=1}^d \exp(\beta \cdot Var_m)}, \quad (12)$$

where the variance term Var_l measures novelty in the l -th feature dimension. Similar to CA1's strong mismatch response to unexpected changes (e.g., a cat on the shoe cabinet), higher variance signals greater deviation from expected patterns within the hyperedge. Such dimensions are deemed more novel and receive larger attention weights g_l , enabling the model to focus on informative atypical features. The parameter β controls sensitivity to these deviations.

$$s_i = \sum_{l=1}^d g_l \cdot (h_{i,l} - \mu_{e,l})^2, \quad (13)$$

$$m_i = \sum_{j \in e \setminus i} \alpha_j \cdot Wh_j, \quad (14)$$

where s_i represents the novelty score of node i , and α_j is the normalized novelty score derived from s_j ; $h_{i,l}$ is the l -th feature dimension of node i , and $\mu_{e,l}$ denotes the l -th dimension of the hyperedge center. In addition, the term m_i denotes the aggregated message passed to node i .

The update process of CNHL can be defined as follows:

$$h'_i = \text{Sigmoid}(h_i + m_i). \quad (15)$$

The process of HCDP and CNHL is presented in Algorithm 1.

Algorithm 1 Brain-inspired fraud detection mechanisms

Input: Constructed multi-view hypergraph \mathcal{G} .
Output: Embedding result h'_i for node i in each view.

```

// Cross-view discrepancy perception
1: for each node  $i \in \mathcal{V}$  do:
2:   for each unordered view pair  $(a_j, a_k)$ ,  $j < k$  do:
3:      $ID\_Diff_i^{(a_1, a_2)} = 1 - \frac{|N_i^{a_1} \cap N_i^{a_2}|}{|N_i^{a_1} \cup N_i^{a_2}|}$ ;
4:     Compute  $Feat\_Diff_i^{(a_1, a_2)}$  by Eqs. (5) and (6);
5:     Obtain  $Label\_Diff_i^{(a_1, a_2)}$  by Eqs. (7) and (8);
6:   end for
7:   Obtain the enhanced  $h_i$  by concatenating the three
      differences with original features  $x_i$  by Eq. (9);
8: end for
// Novelty-aware hypergraph neural network
9: for  $n \leftarrow 1$  to  $N$  do: // The layer of hypergraph
10:   for each node  $i \in \mathcal{V}$  do:
11:     Compute the hyperedge center  $\mu_e$ ;
12:     Compute the novelty weight  $g_l$ ;
13:      $s_i = \sum_{l=1}^d g_l \cdot (h_{i,l} - \mu_{e,l})^2$ ; // Novelty score
14:     Obtain the aggregated message by Eq. (14);
15:     Update node embedding by Eq. (15);
16:   end for
17: end for

```

4.4 Multi-View Hypergraph Fusion

In this section, we perform weighted fusion of transaction node embeddings from different views for Multi-view Hypergraph Fusion (MHF), followed by a downstream fraud detection task. This allows the model to integrate complementary information across heterogeneous perspectives.

$$\alpha_{\mathcal{A}} = \text{Softmax}(W_g \cdot \text{Relu}(\text{Concat}[h'_{a_1}, h'_{a_2}, \dots, h'_{a_{|\mathcal{A}|}}])), \quad (16)$$

where $h'_{a_1}, h'_{a_2}, \dots, h'_{a_{|\mathcal{A}|}}$ denote the hypergraph-learned embeddings of a transaction node under each view, and $\alpha_{\mathcal{A}}$ represents the attention weights across views, used to adaptively fuse multi-view representations.

$$\delta\alpha_{\mathcal{A}}^{(a)} = \text{MLP}^{(a)}(\text{Tanh}(W_p \cdot \sum_{a \in \mathcal{A}} h'^{(a)})), \quad (17)$$

where $\delta\alpha_{\mathcal{A}}^{(a)}$ represents the view-specific modulation term, used to refine the final fusion weights.

$$h'^{final} = \sum_{a=1}^{|\mathcal{A}|} \frac{\alpha_{\mathcal{A}}^{(a)} + \delta\alpha_{\mathcal{A}}^{(a)}}{\sum_{j=1}^{|\mathcal{A}|} (\alpha_{\mathcal{A}}^{(j)} + \delta\alpha_{\mathcal{A}}^{(j)})} \cdot h'^{(a)}, \quad (18)$$

where the final fused representation h'^{final} is obtained via a reweighted combination across views, with modulation-enhanced attention normalized across all views. Here, $\alpha_{\mathcal{A}}^{(a)} + \delta\alpha_{\mathcal{A}}^{(a)}$ denotes the adjusted view weight after modulation, which is normalized to derive the final view-level attention.

The representation h'^{final} serves as the input to the final classifier. The classifier is a lightweight MLP, which includes a linear transformation, followed by batch normalization, activation, dropout, and another linear transformation. HIMVH is trained end-to-end, with the classification cross-entropy loss guiding the optimization of all components.

5 Experiments

5.1 Experimental Setup

Datasets. We conduct experiments on six financial fraud datasets that reflect real risks faced by online users, including two public and four private datasets. These datasets represent fraud patterns that threaten societal fairness and the security of web-based financial ecosystems. The statistical details are summarized in Table 1.

Table 1: Statistics of six datasets.

Dataset	#Record	#Fraud	#Legitimate	#Unlabeled
S-FFSD	77,881	5,256	24,387	48,238
Sparkov	99,728	298	29,620	69,810
Private-1	666,592	10,478	56,181	599,933
Private-2	691,661	609	33,974	657,078
Private-3	264,807	313	39,408	225,086
Private-4	1,243,035	324	49,397	1,193,314

Table 2: Fraud detection performance on six datasets compared with 15 SOTA models.

Types	Models	S-FFSD			Sparkov			Private-1		
		AUC	F1	AP	AUC	F1	AP	AUC	F1	AP
Traditional	Decision Tree	0.6771	0.7276	0.4551	0.6712	0.7454	0.3124	0.8569	0.8527	0.6028
	XGBoost	0.6961	0.7488	0.4873	0.6782	0.7505	0.3154	0.8654	0.8691	0.6421
Deep learning	MCNN	0.7550	0.6481	0.3285	0.8617	0.6526	0.1562	0.9350	0.8877	0.6870
	STAN	0.7682	0.7209	0.3852	0.8890	0.6379	0.1491	0.9336	0.8716	0.6527
Graph learning	PNA	0.6973	0.6348	0.2911	0.8604	0.7859	0.3509	0.9126	0.8114	0.4852
	STAGN	0.8003	0.7401	0.4172	0.9458	0.8355	0.5103	0.9462	0.8983	0.7137
	PC-GNN	0.8544	0.7031	0.6937	0.9253	0.5505	0.3957	0.9775	0.8617	0.8507
	BWGNN	0.8728	0.7278	0.7166	0.9659	0.8398	0.7866	0.9818	0.9100	0.8657
	GHRN	0.8744	0.7204	0.7212	0.9752	0.8499	0.7882	0.9817	0.9127	0.8642
	GTAN	0.8286	0.7336	0.6585	0.9624	0.7774	0.6422	0.9829	0.9289	0.8819
	U-A2GAD	0.8570	0.7682	0.7007	0.9494	0.8249	0.6736	0.9769	0.9149	0.8532
	ConsisGAD	0.7218	0.7173	0.5535	0.8801	0.6891	0.3554	0.9783	0.9144	0.8588
	UniGAD	0.8492	0.7629	0.6918	0.9689	0.8157	0.6223	0.9825	0.9265	0.8757
	RGTAN	0.8461	0.7513	0.6939	0.9581	0.8143	0.6722	0.9837	0.9251	0.8943
	SpaceGNN	0.8655	0.7589	0.7027	0.9762	0.8527	0.7999	0.9809	0.9207	0.8724
	HIMVH	0.8883	0.7874	0.7356	0.9821	0.9379	0.8776	0.9864	0.9291	0.9061
Types	Models	Private-2			Private-3			Private-4		
		AUC	F1	AP	AUC	F1	AP	AUC	F1	AP
Traditional	Decision Tree	0.8924	0.8732	0.5699	0.8575	0.8451	0.4825	0.7642	0.7904	0.3468
	XGBoost	0.7631	0.8185	0.4416	0.8123	0.8321	0.4492	0.7479	0.7956	0.3692
Deep learning	MCNN	0.9631	0.8880	0.6278	0.9319	0.8119	0.4286	0.9649	0.7980	0.4140
	STAN	0.9622	0.8405	0.5116	0.9325	0.8139	0.4330	0.9307	0.7825	0.3687
Graph learning	PNA	0.9663	0.8422	0.5177	0.8893	0.8309	0.4575	0.8599	0.7832	0.3447
	STAGN	0.9864	0.8220	0.4839	0.9221	0.7941	0.3893	0.9365	0.7781	0.3629
	PC-GNN	0.9824	0.6761	0.7139	0.9576	0.6872	0.4377	0.9860	0.5723	0.5869
	BWGNN	0.9852	0.8576	0.7914	0.9749	0.7360	0.5347	0.9862	0.7481	0.5631
	GHRN	0.9879	0.8763	0.7957	0.9621	0.7813	0.5270	0.9651	0.7914	0.5675
	GTAN	0.9829	0.8793	0.7989	0.9867	0.8560	0.7556	0.9656	0.7908	0.6435
	U-A2GAD	0.9744	0.8710	0.6929	0.9868	0.8023	0.5176	0.9748	0.7696	0.4501
	ConsisGAD	0.9769	0.8721	0.6456	0.9723	0.7859	0.3857	0.9638	0.7672	0.3692
	UniGAD	0.9900	0.8171	0.7861	0.9849	0.8158	0.6726	0.9805	0.7897	0.5278
	RGTAN	0.9863	0.8635	0.7952	0.9816	0.8350	0.7139	0.9744	0.7888	0.6416
	SpaceGNN	0.9893	0.8763	0.8160	0.9845	0.8534	0.7599	0.9714	0.7759	0.5642
	HIMVH	0.9917	0.9045	0.8568	0.9936	0.8634	0.7882	0.9900	0.8432	0.7228

Xiang et al. [45] collect online records from collaborated partners and names it as S-FFSD¹. The Sparkov² dataset is publicly available, with a record of transactions of 100 customers from February 1, 2023, to March 31, 2023. We employ a dataset of web finance transaction records provided by a financial institution as Private, spanning from January to April. The subsets labeled as Private-1 to Private-4 correspond to the online transaction data of each month. In addition to identity-related attributes of the transaction parties, each private dataset includes eight attribute features, such as indicators of IP address legitimacy, transaction timestamps, and other behavioral information. Detailed attribute information of the Private dataset can be found in Figure 7.

¹<https://github.com/AI4Risk/antifraud>

²<https://github.com/Namebrandon/Sparkov>

Baselines. We employ 15 SOTA models, which are mainly divided into three categories. Decision Tree [48] and XGBoost [25] are traditional models, MCNN [8] and STAN [5] are deep learning models without graph learning, while PNA [49], STAGN [4], PC-GNN [21], BWGNN [32], GHRN [9], GTAN [45], U-A2GAD [18], ConsisGAD [3], UniGAD [19], RGTAN [44], and SpaceGNN [7] are graph learning models.

Evaluation Metrics and Implementation Details. We utilize area under curve (AUC), macro average of F1 score (F1), average precision (AP) to evaluate the effectiveness of our model. We implement HIMVH using PyTorch 1.13.1 and conduct all experiments on a server equipped with an NVIDIA V100 (32GB), Intel Xeon Gold 6230 CPUs. We employ the Adam optimizer with a learning rate of 0.001 and train the model for 50 epochs. We set batch size and hidden dimension to 512 and 256, respectively. The train, validation and test ratios are set to 60%, 10%, 30%, respectively. In particular,

the number of views is 4, and the number of GNN layers is 3. Furthermore, the size of the temporal sliding window w is set to 4, and novelty-sensitivity parameter β is set to 1.

5.2 Overall Results

We comprehensively evaluate the detection performance of different models, and the results are shown in Table 2.

HIMVH consistently outperforms all baselines across six datasets in terms of three metrics. Compared with other graph learning baselines, HIMVH achieves average gains of 3.32% in AUC, 9.36% in F1 score, and 27.80% in AP, confirming its superior generalization capability and effectiveness. These improvements stem from two components. HCDP detects latent inconsistencies in fraud across multiple views, effectively addressing the heterogeneity of camouflaged patterns. Meanwhile, CNHL captures deviations from local neighborhood predictions, enhancing the representation of sparse minority instances under tail regions.

Even on highly imbalanced datasets such as Private-3 and Private-4, HIMVH outperforms all baselines by at least 3.72% and 12.32% in AP, respectively. This advantage is largely attributed to the heterophily-aware graph learning in HIMVH, which enables more accurate message aggregation across dissimilar nodes and enhances the detection of underrepresented fraudulent patterns.

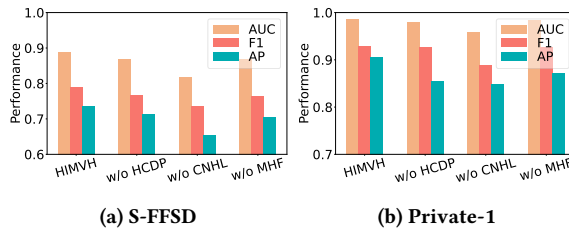


Figure 4: The ablation analysis on S-FFSD and Private-1.

5.3 Ablation Study

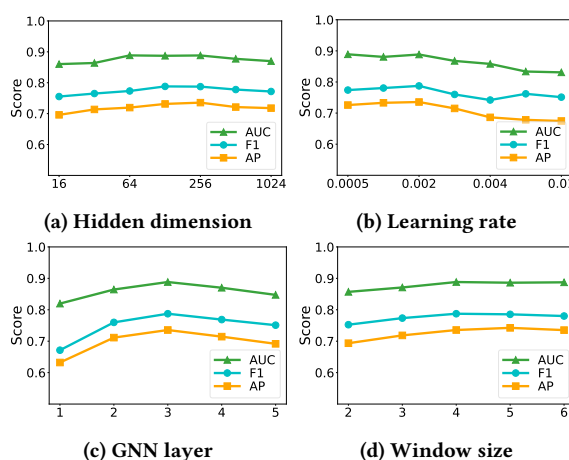


Figure 5: Parameter sensitivity analysis.

To examine the contribution of key design in HIMVH, we conduct ablation studies on three variants:

- **w/o HCDP:** We remove the Hippocampal Cross-view Discrepancy Perception module.
- **w/o CNHL:** The component of CA1-inspired Novelty-aware Hypergraph Learning is replaced with multi-head attention mechanism.
- **w/o MHF:** We remove the Multi-view Hypergraph Fusion module and report the average classification performance across individual views as the final result.

As shown in Figure 4, HIMVH outperforms all three ablated variants, demonstrating the effectiveness of its core components. Specifically, the performance drops observed in w/o HCDP and w/o MHF confirm the importance of multi-view hypergraph modeling, particularly the role of cross-view inconsistency detection in uncovering camouflaged online fraudulent behaviors. Moreover, HIMVH w/o CNHL yields the poorest performance, as the heterophily-aware graph learning mechanism in HIMVH enables more adaptive and discriminative message propagation across structurally diverse nodes, which is critical for capturing minority fraud patterns under long-tailed distributions.

5.4 Sensitivity Analysis

To assess the robustness of HIMVH, we conduct a comprehensive sensitivity analysis on four key hyperparameters.

As shown in Figure 5, HIMVH maintains stable performance across various hyperparameter settings, highlighting its robustness. Specifically, Figure 5 (c) shows that shallow GNNs underfit due to limited receptive fields and insufficient structural information propagation, while deeper models (4–5 layers) avoid significant degradation, attributed to CNHL, which functions as a heterophily-aware graph learning paradigm and mitigate over-smoothing encountered in deeper GNNs. Figure 5 (d) further indicates that performance improves with larger temporal window sizes, then plateaus, as small windows w restrict temporal context required for modeling hyperedge center.

5.5 Visualization and Interpretability Analysis

To assess the effectiveness of HIMVH, we utilize t-SNE [35] on different graph learning models. Specifically, we conduct experiments on the Private-4 dataset. Due to the extreme class imbalance, we visualize all fraud samples along with 10% of the normal samples to ensure a clearer and more informative representation. The visualization results of eight SOTA models are presented in Figure 6, where red nodes represent online fraud behaviors and green nodes denote online normal behaviors. Although models (a)–(g) achieve commendable decoupling effects, some red nodes still appear within green regions. In contrast, HIMVH model demonstrates superior decoupling performance in distinguishing between normal and fraud nodes, as evidenced by the clear separation of red and green points in the embedding visualization. This suggests that HIMVH is more effective in capturing underlying fraud patterns and learning discriminative representations compared to existing models.

We further perform SHAP [22] analysis to enhance model interpretability (Figure 7). The color gradient from blue to red indicates increasing feature values, and features higher on the vertical axis

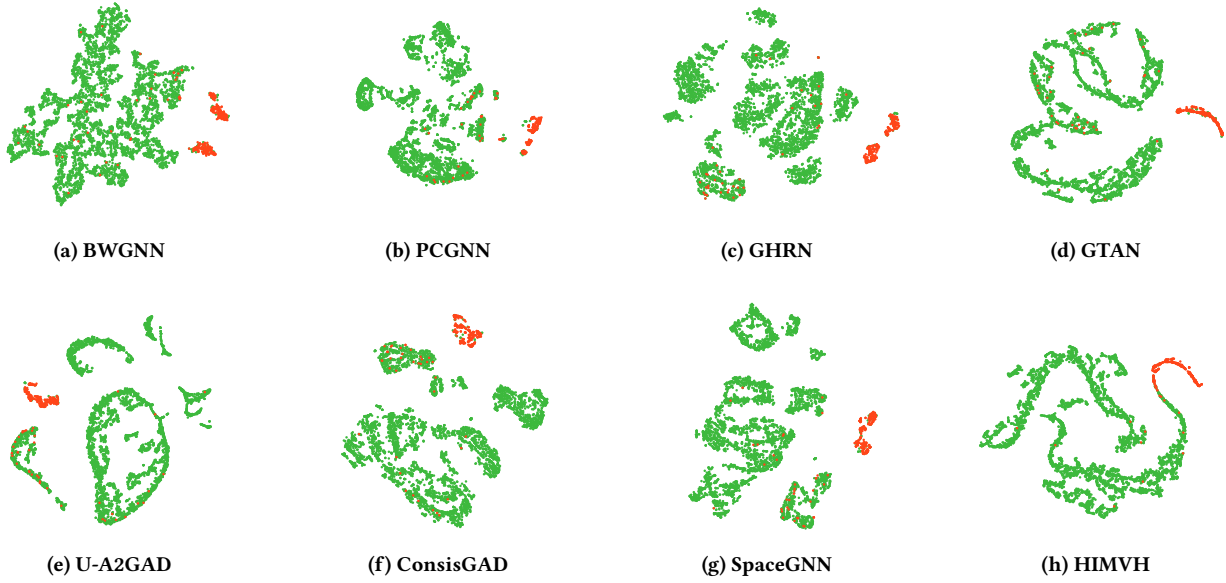


Figure 6: Embedding visualization of different models.

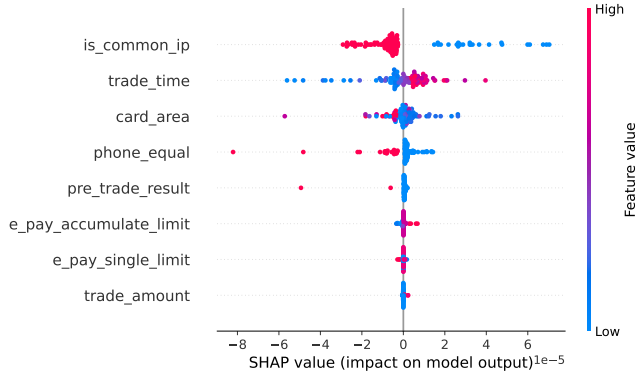


Figure 7: SHAP analysis on Private-4.

contribute more to the model's decisions. The 'is_common_ip' feature stands out: blue dots (uncommon IPs) are associated with higher SHAP values, indicating greater fraud risk. This aligns with fraud patterns in which attackers often use ephemeral or rarely seen IP addresses to avoid being linked to known benign user behavior, thereby evading IP-based detection heuristics. Our SHAP-based analysis illustrates how the distributional discrepancies of different features influence the decision boundaries learned by HIMVH.

5.6 Discussion

We conduct a comparative analysis of several graph-based web finance fraud detection models and provide an explanation that improves interpretability, thereby supporting safer web financial environments and advancing broader social good.

GTAN, though equipped with temporal attention, applies a uniform aggregation and static embeddings, and fails to capture semantic inconsistencies. U-A2GAD adopts fixed kNN-based graph construction and polynomial spectral filtering, which restrict its adaptability to local structural variations. As a result, it struggles to respond to behavioral inconsistencies and camouflaged fraud patterns that deviate from the dominant transactional structure. ConsisGAD emphasizes consistency regularization under low supervision but underutilizes labeled data. This weakens its discriminative power in complex scenarios, and boundaries where fraud is sparse and ambiguous. UniGAD unifies multi-level tasks through subgraph sampling and a shared fusion module. However, its sampler prioritizes nodes with pronounced signals while discarding neighbors that appear normal yet convey essential relational cues. This bias narrows the retrieved subgraphs and limits the UniGAD's capability to capture full anomaly contexts.

While RGTAN, and SpaceGNN perform well by modeling temporal patterns or alleviating label sparsity, they lack explicit mechanisms for identifying camouflaged fraud that mimics normal behavior and for capturing rare fraudulent activities situated at the periphery of the data distribution. These limitations reduce their effectiveness in scenarios where subtle behavioral inconsistencies and low-frequency fraud signals are critical for accurate detection.

6 Conclusion

In this work, we propose HIMVH, a hippocampus-inspired multi-view hypergraph learning framework tailored for web finance fraud detection. Inspired by hippocampus's scene conflict detection mechanism, we propose hippocampal cross-view discrepancy perception module. Specifically, we quantify the behavioral discrepancies of the same online transaction across different views, capturing

latent cross-view conflicts from multiple dimensions to characterize camouflaged patterns more comprehensively. In addition, inspired by the match–mismatch novelty detection mechanism in the hippocampal CA1 region, we propose a heterophily-sensitive graph learning paradigm. This approach employs a deviation-aware message passing strategy, which adaptively reweights node messages based on their divergence from local neighborhood structures, thereby amplifying subtle anomaly signals from rare tail instances. Experimental results on six real-world web finance fraud datasets show that HIMVH achieves 6.42% improvement in AUC, 9.74% in F1 and 39.14% in AP on average over 15 SOTA models.

In future, we plan to extend HIMVH to broader fraud detection scenarios beyond web finance domain, including but not limited to fake news dissemination and identity fraud.

References

- [1] Seyyede Zahra Aftabi, Ali Ahmadi, and Saeed Farzi. 2023. Fraud detection in financial statements using data mining and GAN models. *Expert Systems with Applications* 227 (2023), 120144.
- [2] Katie C Bittner, Christine Grienberger, Sachin P Vaidya, Aaron D Milstein, John J Macklin, Junghyup Suh, Susumu Tonegawa, and Jeffrey C Magee. 2015. Conjunctive input processing drives feature selectivity in hippocampal CA1 neurons. *Nature neuroscience* 18, 8 (2015), 1133–1142.
- [3] Nan Chen, Zemin Liu, Bryan Hooi, Bingsheng He, Rizal Fathony, Jun Hu, and Jia Chen. 2024. Consistency training with learnable data augmentation for graph anomaly detection with limited supervision. In *The Twelfth International Conference on Learning Representations*.
- [4] Dawei Cheng, Xiaoyang Wang, Ying Zhang, and Liqing Zhang. 2020. Graph neural network for fraud detection via spatial-temporal attention. *IEEE Transactions on Knowledge and Data Engineering* 34, 8 (2020), 3800–3813.
- [5] Dawei Cheng, Sheng Xiang, Chencheng Shang, Yiyi Zhang, Fangzhou Yang, and Liqing Zhang. 2020. Spatio-temporal attention-based neural network for credit card fraud detection. In *Proceedings of the AAAI conference on artificial intelligence*, Vol. 34. 362–369.
- [6] Dawei Cheng, Yujia Ye, Sheng Xiang, Zhenwei Ma, Ying Zhang, and Changjun Jiang. 2023. Anti-Money Laundering by Group-Aware Deep Graph Learning. *IEEE Transactions on Knowledge and Data Engineering* 35, 12 (2023), 12444–12457. doi:10.1109/TKDE.2023.3272396
- [7] Xiangyu Dong, Xingyi Zhang, Lei Chen, Mingxuan Yuan, and Sibo Wang. 2025. SpaceGNN: Multi-Space Graph Neural Network for Node Anomaly Detection with Extremely Limited Labels. *arXiv preprint arXiv:2502.03201* (2025).
- [8] Kang Fu, Dawei Cheng, Yi Tu, and Liqing Zhang. 2016. Credit card fraud detection using convolutional neural networks. In *Neural Information Processing: 23rd International Conference, ICONIP 2016, Kyoto, Japan, October 16–21, 2016, Proceedings, Part III* 23. Springer, 483–490.
- [9] Yuan Gao, Xiang Wang, Xiangnan He, Zhenguang Liu, Huamin Feng, and Yongdong Zhang. 2023. Addressing heterophily in graph anomaly detection: A perspective of graph spectrum. In *Proceedings of the ACM Web Conference 2023*. 1528–1538.
- [10] Mingjian Guang, Zhong Li, Chungang Yan, Yuhua Xu, Junli Wang, Dawei Cheng, and Changjun Jiang. 2025. Multi-Temporal Partitioned Graph Attention Networks for Financial Fraud Detection. *IEEE Transactions on Information Forensics and Security* (2025).
- [11] Venus Haghhighi, Behnaz Soltani, Nasrin Shabani, Jia Wu, Yang Zhang, Lina Yao, Quan Z Sheng, and Jian Yang. 2024. TROPICAL: Transformer-based Hypergraph Learning for Camouflaged Fraudster Detection. In *2024 IEEE International Conference on Data Mining (ICDM)*. IEEE, 121–130.
- [12] Li Han, Longxun Wang, Ziyang Cheng, Bo Wang, Guang Yang, Dawei Cheng, and Xuemin Lin. 2025. Mitigating the Tail Effect in Fraud Detection by Community Enhanced Multi-Relation Graph Neural Networks. *IEEE Transactions on Knowledge and Data Engineering* (2025).
- [13] Mengda Huang, Yang Liu, Xiang Ao, Kuan Li, Jianfeng Chi, Jinghua Feng, Hao Yang, and Qing He. 2022. Auc-oriented graph neural network for fraud detection. In *Proceedings of the ACM web conference 2022*. 1311–1321.
- [14] Joshua B Julian and Christian F Doeller. 2021. Remapping and realignment in the human hippocampal formation predict context-dependent spatial behavior. *Nature neuroscience* 24, 6 (2021), 863–872.
- [15] Abdullah Lakhan, Mazin Abed Mohammed, Dheyaa Ahmed Ibrahim, Seifedine Kadry, and Karrar Hameed Abdulkareem. 2022. ITS based on deep graph convolutional fraud detection network blockchain-enabled fog-cloud. *IEEE Transactions on Intelligent Transportation Systems* 24, 8 (2022), 8399–8408.
- [16] B. Lebichot, W. Siblini, G.M. Paldino, Y.-A. Le Borgne, F. Oblé, and G. Bontempi. 2024. Assessment of catastrophic forgetting in continual credit card fraud detection. *Expert Systems with Applications* 249 (2024), 123445. doi:10.1016/j.eswa.2024.123445
- [17] Xiangfeng Li, Shenghua Liu, Zifeng Li, Xiaotian Han, Chuan Shi, Bryan Hooi, He Huang, and Xueqi Cheng. 2020. FlowScope: Spotting Money Laundering Based on Graphs. *Proceedings of the AAAI Conference on Artificial Intelligence* 34 (04 2020), 4731–4738. doi:10.1609/aaai.v34i04.5906
- [18] Yuqi Li, Guosheng Zang, Chunyue Song, and Xiaojie Yuan. 2025. A universal adaptive algorithm for graph anomaly detection. *Information Processing & Management* 62, 1 (2025), 103905.
- [19] Yiqing Lin, Jianheng Tang, Chenyi Zi, H Vicky Zhao, Yuan Yao, and Jia Li. 2024. UniGAD: Unifying Multi-level Graph Anomaly Detection. *arXiv preprint arXiv:2411.06427* (2024).
- [20] Junyi Liu, Dawei Cheng, and Changjun Jiang. 2023. Preventing Attacks in Interbank Credit Rating with Selective-aware Graph Neural Network. In *IJCAI*. 6085–6093.
- [21] Yang Liu, Xiang Ao, Zidi Qin, Jianfeng Chi, Jinghua Feng, Hao Yang, and Qing He. 2021. Pick and choose: a GNN-based imbalanced learning approach for fraud detection. In *Proceedings of the web conference 2021*. 3168–3177.
- [22] Scott M. Lundberg and Su-In Lee. 2017. A Unified Approach to Interpreting Model Predictions. In *Neural Information Processing Systems*. <https://api.semanticscholar.org/CorpusID:21889700>
- [23] Xuejiao Luo, Xiaohui Han, Wenbo Zuo, Xiaoming Wu, and Wenyin Liu. 2024. MLAd²: A Semi-Supervised Money Laundering Detection Framework Based on Decoupling Training. *IEEE Transactions on Information Forensics and Security* 19 (2024), 4518–4533. doi:10.1109/TIFS.2024.3380262
- [24] Jiacheng Ma, Fan Li, Rui Zhang, Zhikang Xu, Dawei Cheng, Yi Ouyang, Ruihui Zhao, Jianguang Zheng, Yefeng Zheng, and Changjun Jiang. 2023. Fighting against Organized Fraudsters Using Risk Diffusion-based Parallel Graph Neural Network. In *IJCAI*. 6138–6146.
- [25] Isaac Kofi Nti and Arjun Remadevi Somanathan. 2022. A scalable RF-XGBoost framework for financial fraud mitigation. *IEEE Transactions on Computational Social Systems* 11, 2 (2022), 1556–1563.
- [26] Maxx Richard Rahman, Lotfy Abdel Khaliq, Thomas Piper, Hans Geyer, Tristan Equey, Norbert Baume, Reid Aikin, and Wolfgang Maass. 2024. SACNN: self attention-based convolutional neural network for fraudulent behaviour detection in sports. In *Proceedings of the Thirty-Third International Joint Conference on Artificial Intelligence*. 6017–6025.
- [27] Y Sahin and Ekrem Duman. 2011. Detecting credit card fraud by decision trees and support vector machines. In *Proceedings of the International MultiConference of Engineers and Computer Scientists*, Vol. 1. 1–6.
- [28] Haolun Shi, Mohammad A. Tayebi, Jian Pei, and Jiguo Cao. 2023. Cost-Sensitive Learning for Medical Insurance Fraud Detection With Temporal Information . *IEEE Transactions on Knowledge & Data Engineering* 35, 10 (Oct. 2023), 10451–10463. doi:10.1109/TKDE.2023.3240431
- [29] Ajeet Singh, Anurag Jain, and Seblewongel Esseynew Biable. 2022. Financial fraud detection approach based on firefly optimization algorithm and support vector machine. *Applied Computational Intelligence and Soft Computing* 2022, 1 (2022), 1468015.
- [30] Emilia Strelcenia and Simant Pakoonwit. 2023. Improving Classification Performance in Credit Card Fraud Detection by Using New Data Augmentation. *AI* 4 (01 2023), 172–198. doi:10.3390/ai4010008
- [31] Jianheng Tang, Fengrui Hua, Ziqi Gao, Peilin Zhao, and Jia Li. 2023. Gadbench: Revisiting and benchmarking supervised graph anomaly detection. *Advances in Neural Information Processing Systems* 36 (2023), 29628–29653.
- [32] Jianheng Tang, Jiajin Li, Ziqi Gao, and Jia Li. 2022. Rethinking graph neural networks for anomaly detection. In *International Conference on Machine Learning*. PMLR, 21076–21089.
- [33] Yue Tian, Guanjun Liu, Jiacun Wang, and Mengchu Zhou. 2023. ASA-GNN: Adaptive Sampling and Aggregation-Based Graph Neural Network for Transaction Fraud Detection. *IEEE Transactions on Computational Social Systems* (2023).
- [34] Rafael Van Belle, Bart Baesens, and Jochen De Weerdt. 2023. CATCHM: A novel network-based credit card fraud detection method using node representation learning. *Decision Support Systems* 164 (2023), 113866. doi:10.1016/j.dss.2022.113866
- [35] Laurens Van der Maaten and Geoffrey Hinton. 2008. Visualizing data using t-SNE. *Journal of machine learning research* 9, 11 (2008).
- [36] Chenxu Wang, Mengqin Wang, Xiaoguang Wang, Luyue Zhang, and Yi Long. 2024. Multi-Relational graph Representation learning for financial statement fraud detection. *Big Data Mining and Analytics* 7, 3 (2024), 920–941.
- [37] Daixin Wang, Jianbin Lin, Peng Cui, Quanhui Jia, Zhen Wang, Yanming Fang, Quan Yu, Jun Zhou, Shuang Yang, and Yuan Qi. 2019. A semi-supervised graph attentive network for financial fraud detection. In *2019 IEEE international conference on data mining (ICDM)*. IEEE, 598–607.
- [38] Shuhao Wang, Cancheng Liu, Xiang Gao, Hongtao Qu, and Wei Xu. 2017. Session-Based Fraud Detection in Online E-Commerce Transactions Using Recurrent Neural Networks. In *Machine Learning and Knowledge Discovery in Databases*,

- Yasemin Altun, Kamalika Das, Taneli Mielikäinen, Donato Malerba, Jerzy Stefanowski, Jesse Read, Marinka Žitnik, Michelangelo Ceci, and Sašo Džeroski (Eds.). Springer International Publishing, Cham, 241–252.
- [39] Xin Wang, Luo Xiangfeng, Xinzh Wang, and Hang Yu. 2024. Homophilic and Heterophilic-Aware Sparse Graph Transformer for Financial Fraud Detection. In *2024 International Joint Conference on Neural Networks (IJCNN)*. 1–8. doi:10.1109/IJCNN60899.2024.10650212
- [40] Bin Wu, Xinyu Yao, Boyan Zhang, Kuo-Ming Chao, and Yinsheng Li. 2023. Split-GNN: Spectral Graph Neural Network for Fraud Detection against Heterophily. In *Proceedings of the 32nd ACM International Conference on Information and Knowledge Management*. 2737–2746.
- [41] Jiasheng Wu, Xin Liu, Dawei Cheng, Yi Ouyang, Xian Wu, and Yefeng Zheng. 2024. Safeguarding fraud detection from attacks: A robust graph learning approach. In *Proceedings of the 33rd International Joint Conference on Artificial Intelligence*. 7500–7508.
- [42] Yanxi Wu, Liping Wang, Hongyu Li, and Jizhao Liu. 2025. A Deep Learning Method of Credit Card Fraud Detection Based on Continuous-Coupled Neural Networks. *Mathematics* 13 (02 2025), 819. doi:10.3390/math13050819
- [43] Huosong Xia, Wuyue An, and Zuopeng Justin Zhang. 2023. Credit risk models for financial fraud detection: A new outlier feature analysis method of xgboost with smote. *Journal of Database Management (JDM)* 34, 1 (2023), 1–20.
- [44] Sheng Xiang, Guibin Zhang, Dawei Cheng, and Ying Zhang. 2025. Enhancing Attribute-Driven Fraud Detection With Risk-Aware Graph Representation. *IEEE Transactions on Knowledge and Data Engineering* (2025).
- [45] Sheng Xiang, Mingzhi Zhu, Dawei Cheng, Enxia Li, Ruihui Zhao, Yi Ouyang, Ling Chen, and Yefeng Zheng. 2023. Semi-supervised credit card fraud detection via attribute-driven graph representation. In *Proceedings of the AAAI Conference on Artificial Intelligence*, Vol. 37. 14557–14565.
- [46] Fei Xiao, Shaofeng Cai, Gang Chen, HV Jagadish, Beng Chin Ooi, and Meihui Zhang. 2024. VecAug: Unveiling Camouflaged Frauds with Cohort Augmentation for Enhanced Detection. In *Proceedings of the 30th ACM SIGKDD Conference on Knowledge Discovery and Data Mining*. 6025–6036.
- [47] Yu Xie, Guanjun Liu, Changjun Yan, Changjun Jiang, and MengChu Zhou. 2023. Time-Aware Attention-Based Gated Network for Credit Card Fraud Detection by Extracting Transactional Behaviors. *IEEE Transactions on Computational Social Systems* 10, 3 (2023), 1004–1016. doi:10.1109/TCSS.2022.3158318
- [48] Biao Xu, Yao Wang, Xiuwu Liao, and Kaidong Wang. 2023. Efficient fraud detection using deep boosting decision trees. *Decision Support Systems* 175 (2023), 114037.
- [49] Keyulu Xu, Weihua Hu, Jure Leskovec, and Stefanie Jegelka. 2018. How powerful are graph neural networks? *arXiv preprint arXiv:1810.00826* (2018).
- [50] Xiaolong Xu, Lingjuan Lyu, Yihong Dong, Yicheng Lu, Weiqiang Wang, and Hong Jin. 2023. Splitggn: splitting GNN for node classification with heterogeneous attention. *arXiv preprint arXiv:2301.12885* (2023).
- [51] Jinghui Zhang, Zhengjia Xu, Dingyang Lv, Zhan Shi, Dian Shen, Jiahui Jin, and Fang Dong. 2024. DIG-In-GNN: discriminative feature guided GNN-based fraud detector against inconsistencies in multi-relation fraud graph. In *Proceedings of the AAAI Conference on Artificial Intelligence*, Vol. 38. 9323–9331.
- [52] Yue Zhao and Maciej K Hryniwski. 2018. Xgbd: improving supervised outlier detection with unsupervised representation learning. In *2018 International Joint Conference on Neural Networks (IJCNN)*. IEEE, 1–8.
- [53] Yao Zou and Dawei Cheng. 2025. Effective high-order graph representation learning for credit card fraud detection. *arXiv preprint arXiv:2503.01556* (2025).

A Implementation Details of the Baselines

A.1 Models Without Graph Learning

- **MCNN [8].** MCNN is a fraud detection model, which constructs feature matrix with transaction data. MCNN is the pioneering work that applies convolutional neural networks (CNNs) to financial fraud detection.
- **STAN [5].** STAN employs a spatial-temporal attention mechanism to model transaction records. However, since the datasets utilized in our experiments lack spatial information, we exclude the spatial component from STAN in our implementation.

A.2 Graph Learning Models

- **BWGNN [32].** BWGNN captures abnormal patterns by focusing on high-frequency spectral energy shifts, offering improved detection performance.

- **GHRN [9].** GHRN tackles the heterophily problem in graph by utilizing the smoothness index and graph Laplacian to identify high-frequency components. It employs node predictions to estimate high-frequency signals, and ensures robust identification even with limited labeled data.
- **GTAN [45].** GTAN passes messages among nodes via a gated temporal attention mechanism to learn transaction representations, and model fraud patterns through risk propagation.
- **ConsisGAD [3].** ConsisGAD addresses limited supervision and class imbalance in graph anomaly detection via consistency training and learnable data augmentation, and enhances detection performance by leveraging differences in node homophily distribution within a GNN backbone.
- **RGTAN [44].** RGTAN constructs a temporal transaction graph and uses a gated temporal graph attention mechanism to learn adaptive transaction representations and enhance multi-hop risk structure perception for improved credit card fraud detection.
- **SpaceGNN [7].** SpaceGNN is a multi-space graph neural network for node anomaly detection with extremely limited labels, leveraging learnable space projection and distance-aware propagation.

To adapt the node-level anomaly detection baselines, we employ the same temporal graph construction approach as GTAN in the task of transaction fraud detection. Specifically, we construct the temporal graph by representing individual transaction records as nodes and establishing edges based on the temporal relationships between transactions.

B Details of Private Dataset

The Private dataset is collected by our partner, a major commercial bank, and consists of online customer transaction records. The web-based transactions are chronologically divided into four monthly subsets, from January to April, denoted as Private-1 to Private-4. Each record is associated with one of three label types: ‘0’ indicates a normal transaction, ‘1’ denotes a fraudulent transaction, and ‘2’ represents missing labels.

In addition to the identity information of the sender and receiver, each transaction contains eight attribute features, namely ‘trade_time’, ‘trade_amount’, ‘card_area’, ‘pre_trade_result’, ‘phone_equal’, ‘is_common_ip’, ‘e_pay_single_limit’, and ‘e_pay_accumulate_limit’. Detailed descriptions of these features are as follows:

- **trade_time:** Time of the transaction.
- **trade_amount:** The amount of a single transaction.
- **card_area:** Geographical region associated with the transaction.
- **pre_trade_result:** Outcome of the previous transaction attempt.
- **phone_equal:** Match between transaction and registered phone.
- **is_common_ip:** Whether the IP address is commonly used.
- **e_pay_single_limit:** Limit for single electronic payment.
- **e_pay_accumulate_limit:** Cumulative limit for payments over time.

Table 3: Fraud detection performance (%) on six datasets when temporal window size w is set to 2.

Method	S-FFSD			Sparkov			Private-1			Private-2			Private-3			Private-4		
	AUC	AP	F1	AUC	AP	F1	AUC	AP	F1	AUC	AP	F1	AUC	AP	F1	AUC	AP	F1
HIMVH	87.30	76.24	71.90	97.01	91.51	87.15	98.41	92.70	89.86	98.73	88.44	83.95	99.04	86.11	74.27	98.01	85.51	68.79
GTAN	80.19	73.79	63.37	94.01	68.22	54.37	97.87	92.05	86.49	98.04	87.19	73.11	99.16	67.80	52.35	96.66	77.40	58.18
RGTAN	79.97	71.45	63.40	95.58	81.00	67.01	97.82	80.16	87.31	96.81	86.47	67.46	97.47	80.57	55.05	95.70	80.29	56.22
SpaceGNN	85.97	59.33	65.28	96.12	73.42	75.66	97.63	85.89	84.73	98.70	79.06	77.26	98.29	64.84	65.30	96.36	56.73	51.72

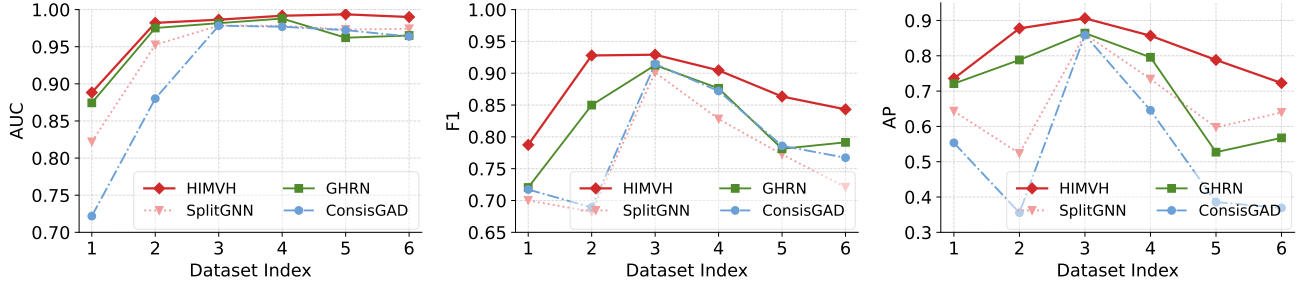


Figure 8: The performance of different heterophily-aware GNN models.

C Additional Experimental Results

C.1 Long-Tail Performance

In this section, to validate the effectiveness of the HIMVH model on the tail portion of the distribution, we set the temporal window w to 2 during graph construction. This choice draws on prior insights [12] and produces a sparse graph in which all nodes fall into the tail region. We assess the model response to tail nodes by comparing the performance drop before and after this change in w . A model with strong robustness to tail nodes should show a small decline in performance.

When the temporal window size w is set to 2, the performance of each model is reported in Table 3. Relative to the original experimental setup, the corresponding performance drop for each model is as follows:

- HIMVH:** HIMVH shows an average drop of 0.80% in AUC, 1.15% in F1, and 2.62% in AP across the six datasets.
- GTAN:** GTAN shows an average drop of 0.87% in AUC, 6.08% in F1, and 11.45% in AP across the six datasets.
- RGTAN:** RGTAN shows an average drop of 1.69% in AUC, 3.59% in F1, and 10.12% in AP across the six datasets.
- SpaceGNN:** HIMVH shows an average drop of 0.64% in AUC, 16.78% in F1, and 6.99% in AP across the six datasets.

Overall, HIMVH records the smallest performance drop among all models. This outcome indicates that HIMVH maintains stable accuracy when all nodes lie in the tail region and sustains reliable results under sparse temporal structures. The consistent performance across six datasets also shows that HIMVH can extract useful signals from nodes with rare patterns and low support. These results confirm the strong capability of HIMVH in tail node analysis, with rare or subtle fraud behaviors.

C.2 Heterophily Analysis

A heterophily-aware GNN refers to a graph model that can capture node relations in graphs where connected nodes often hold different labels or attributes. As a heterophily-aware GNN, HIMVH assigns higher weight to node pairs with larger similarity difference. We compare HIMVH with three heterophily-aware models, SplitGNN [50], GHRN [9], and ConsisGAD [3], where SplitGNN is not part of the 15 SOTA baselines. Figure 8 reports the results on the six datasets in index order from one to six. HIMVH has an average gain of 2.72% in AUC, 14.35% in F1, and 22.26% in AP over SplitGNN. This results confirm the clear advantage of HIMVH over other heterophily aware GNN models.

C.3 Time Efficiency

Table 4: Inference time (s) of different models.

Dataset	Time	Dataset	Time
GTAN	1.44	RGTAN	1.79
HIMVH	2.09	SpaceGNN	3.42

Under the same setup as in the main paper, we assess the inference time on the Private-4 dataset across twenty runs. The inference results appear in Table 4, GTAN costs 1.44 s, RGTAN costs 1.79 s, HIMVH costs 2.09 s, and SpaceGNN costs 3.42 s. These results show that our method secures clearly stronger detection performance while its computational cost remains fully acceptable. The time reported for HIMVH reflects a single forward pass within one view, which indicates that even with its richer feature use and higher accuracy, the overall expense stays well within a practical range for real fraud analysis scenarios.